EXPERIMENTAL STUDY OF A SEISMICALLY ISOLATED BUILDING STRUCTURE SUBJECT TO TRIAXIAL GROUND MOTIONS

Jenn-Shin HWANG[1] And Ting-Yu HSU[2]

SUMMARY

Uni-lateral, bi-lateral and tri-axial shaking table tests are conducted to study the seismic response of a three story base-isolated steel structure. The lateral force distribution formulas specified in the design specifications are evaluated experimentally. A method to calculate the lateral force distribution is proposed and experimentally verified. Seismic responses of the test model to the uni-lateral, bi-lateral and tri-axial ground excitations are compared. The effects of vertical ground acceleration on the maximum acceleration of the superstructure and the maximum displacement of the isolation system are investigated. The maximum displacements of the isolation system under bi-lateral and tri-axial ground motions are compared with those determined from the "1.0+0.3" direction combination rule.

INTRODUCTION

In the past two decades, base-isolated structures have been constructed to passively control their seismic response. Extensive studies have been conducted in laboratories to verify and to enhance the design and analysis theories. Numerous shaking table studies for the seismic responses of base-isolated building structures have been performed in the past. Kelly et al. [1980] have conducted shaking table tests of a base-isolated building structure with a fail-safe system on which the superstructure is carried when the bearings are displaced beyond their stability limit. Kelly et al. [1986] have tested a base-isolated rigid block to the roll-over of the lead-rubber bearings. Griffith et al. [1988] have evaluated the effect of column uplift on the seismic response of a base-isolated building. Al-Hussaini et al. [1993] have performed a series of tests on a base-isolated building with the friction pendulum system. Hwang and Ku [1997] have correlated the experimental results of a rigid block isolated by high damping rubber bearings with those predicted by an analytical model. However, these shaking table studies are all limited to uni-lateral or uni-lateral plus vertical ground excitations.

In this study a three story steel structure isolated by lead-rubber bearings and natural rubber bearings will be tested using a three-axis shaking table. Uni-lateral, bi-lateral and tri-axial ground shakings will be used to investigate the seismic responses of the test structure.

2. TEST MODEL AND TEST PROGRAM

A three story base-isolated steel structure shown in Fig. 1 is assumed to be a 0.4-scale model. The superstructure is composed of three moment resisting frames in the longitudinal (X) direction while two exterior steel dual systems together with a central moment resisting frame are designed in the transverse (Y) direction. Smallest locally available rolled sections are selected for the construction of the test structure. The superstructure is originally designed as a fixed-base structure according to the seismic design specifications of building structures.

[1] Professor,, National Taiwan Univ of Science and Tech Nat Center Research on Equake Eng Taiwan. JSH@mail.ntust.edu.tw
[2] 2. Grad Research Asst, Dept of Construction Eng, Natil Taiwan Univ of Science and Tech, P.O. Box 90-130, Taipei, Taiwan
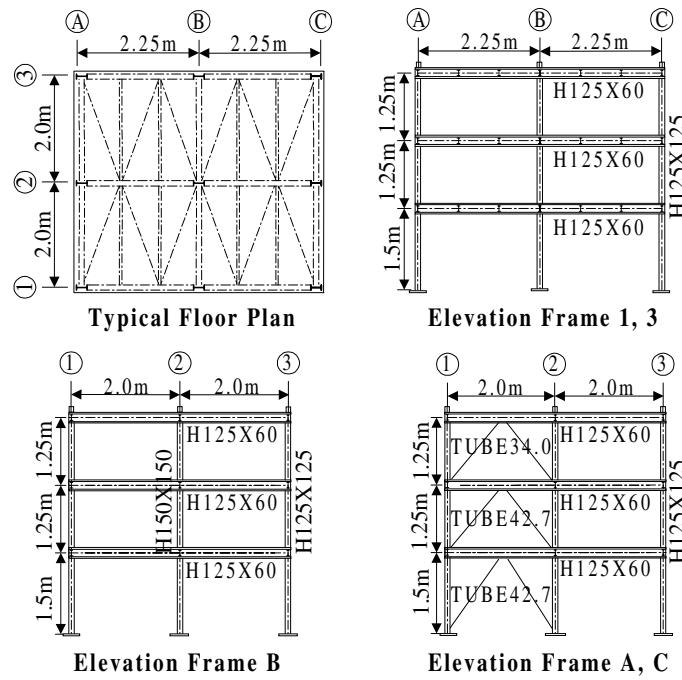
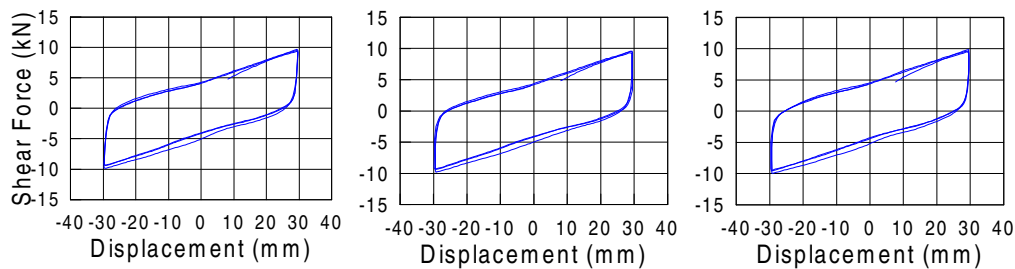Figure 1: Typical plan and elevation of the test superstructure

Figure 2: Typical hysteresis loops from cyclic loading tests

in Taiwan [Seismic 1995], and the reduction of force demand due to the incorporation of the base isolation system is not considered.

Lead bricks weighing $500\,N$ each are attached to the floors of the test model to simulate the seismic reactive mass. The weights from the base floor to the roof are approximately equal to $113\,kN$, $92\,kN$, $92\,kN$, $70\,kN$, respectively. The total weight of the superstructure above the isolation system is estimated to be $367\,kN$.

The isolation system is composed of 8 circular lead-rubber bearings and one natural rubber bearing for the tests. The diameter of the circular lead-rubber bearing is $120\,mm$. The bearing is composed of 16 rubber layers and 15 steel shim plates. The thickness of each rubber layer is $3.5\,mm$ and the thickness of the steel plates is $1\,mm$. The diameter of the lead plug is $25\,mm$. The dimensions of the natural rubber bearings are completely the same as those of the lead-rubber bearings without a lead-core.

Based on the average axial load exerted on the isolation system by the dead load of the superstructure, an axial load of $40\,kN$ is imposed to each bearing for the performance test conducted in a cyclic manner. Very similar hysteresis characteristics have been observed for the entire set of lead-rubber bearings as shown in Fig. 2. Additionally, some other tests are also conducted with a varying axial load. The test results have indicated that the characteristic strength Q_d, effective stiffness K_{eff} and energy dissipation capacity EDC [Guide 1999] of these lead-rubber bearings are dependent on the axial load. This result is consistent with what were reported by Tyler and Robinson [1984].

Six recorded earthquakes shown in Table 1 are used to investigate the three dimensional seismic responses of the test structure. The superstructure and the isolation system are so arranged to yield a symmetric-plan system. Four

tests are conducted for each recorded earthquake. The two horizontal acceleration components of each earthquake are input to the shake table separately in the first two tests, followed by a bi-lateral and a tri-axial excitations. The original time step of 0.02 second of all ground motions is scaled to 0.0125 second according to the scaling factor of the test model.

Table 1: Earthquake records used for shaking table tests

Earthquake Names
100% 1940 Imperial Valley, El Centro, Irrigation Distric, N-S(X), E-W(Y), up(Z)
100% 1980 Loma Prieta, Capitola, Fire Station, $360°$(X), $90°$(Y) and up(Z)
50% 1995 Hanshin, Kobe, JMA Station, N-S(X), E-W(Y) and up(Z)
120% 1989 Loma Prieta,Corralitos, Eureka Canyon Road, $360°$(X), $90°$(Y) and up(Z)
60% 1994 Northridge, New Hall, $360°$(X), $90°$(Y) and up(Z)
200% 1952 Kern Contry, Taft, Lincoln School Tunnel, S69E(X), N21E(Y) and up(Z)

Displacement transducers and accelerometers are installed at the corner and center columns of each story of frame A and frame 3 to measure the seismic responses of the test structure. Nine axial-shear load cells are mounted beneath the isolation bearings to measure the shear forces and to monitor the axial force variation of the bearings.

3. TEST RESULTS
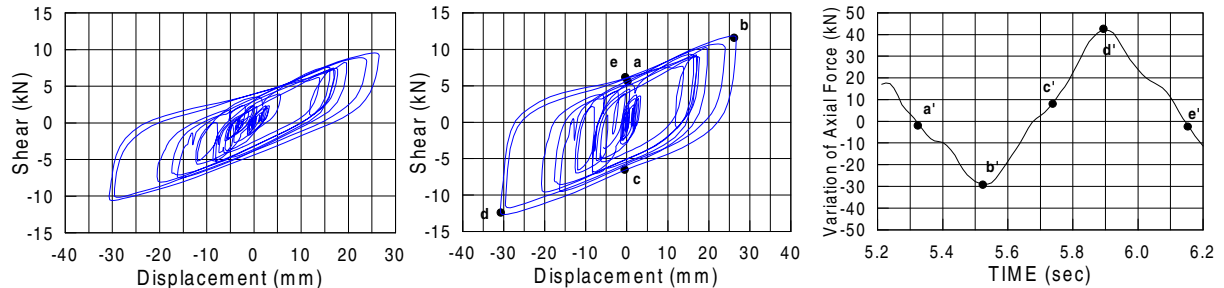
3.1 Uni-lateral Tests

Both the fixed-base and base-isolated conditions of the model are tested using random white noises to determine their natural frequencies. In order not to cause the yielding of the lead-rubber bearings, a small peak ground acceleration of 0.03 g is selected for the white noise ground motion. For the base-isolated condition, the first mode natural frequencies determined from the transfer functions are equal to 2.16 Hz, 4.96 Hz and 12.5 Hz respectively in the longitudinal (X), transverse (Y) and vertical (Z) directions. For the fixed-base model, the first mode natural frequencies are equal to 2.97 Hz and 4.96 Hz corresponding to the longitudinal and transverse directions.

The results from uni-lateral tests indicate that the hysteresis loops of all lead-rubber bearings are not the same or similar to one another. A typical example obtained from the longitudinal test with the Capitola record is shown in Fig. 3 from which it is seen that the EDC, K_{eff} and Q_d of the hysteresis loops are quite different. This result is not the same as what has been observed from the cyclic loading tests in which all lead-rubber bearings reveal very similar hysteresis characteristics. The reason for this difference may be due to the fact that the static axial loads exerting on the bearings under exterior center columns (e.g. the center bearing of frame A) are larger than those on the bearings under corner columns (e.g. the corner bearing of frame A) The average static axial loads exerting on the bearings under the center columns of frames A and C, the center columns of frames 1 and 3, and the corner columns are measured to be equal to 49 kN, 50 kN and 25 kN, respectively. Since the shear force-displacement relationship of the bearings is dependent on the axial load [Tyler and Robinson 1984], the energy dissipation of the bearings under the center columns is larger than that under the corner columns. However, the dependency of the hysteresis loops on the axial load is often not considered in the practical design in which the hysteresis loops of lead-rubber bearings with a same lead core diameter and bearing dimension are usually presumed to be the same. The UBC [uniform 1997] has required design engineers to consider the effect of axial load when modeling the behavior of

isolation bearings for a dynamic time history analysis. However, difficulties arise from the fact that the lead-rubber bearings from different manufacturing processes or manufacturers may reveal different axial load dependency. From this investigation, it is concluded that the effect of the axial load on isolation bearings installed at different locations of a base-isolated structure should be considered for practical design.

In addition to the aforementioned, the hysteresis loop of each bearing shown in Fig. 3 is not skew-symmetric as what has been seen from the cyclic loading test result. This is because the overturning moment of the superstructure undergoing a ground excitation has introduced an axial load variation into the bearings. For example, discrepancy is observed between the traces a - b - c and c - d - e of the hysteresis loops of the center

bearing of frame A as shown in Fig 3(b). Corresponding to these two loop traces, the axial load on the bearing is varying from traces $a^{'} \text{-} b^{'} \text{-} c^{'}$ to $c^{'} \text{-} d^{'} \text{-} e^{'}$ as shown in Fig.3(c). Since the loading variation trace $c^{'} \text{-} d^{'} \text{-} e^{'}$ shows an increase on the compressive axial load while the load loading variation trace $a^{'} \text{-} b^{'} \text{-} c^{'}$ depicts a decrease on the compressive axial load, the area encased in the loop trace $c \text{-} d \text{-} e$ is larger than that covered by the loop trace $a \text{-} b \text{-} c$. The effect of axial load induced by the overturning of the superstructure should also be considered in the practical analysis.

Figure 3: (a) Hysteresis loops of corner bearing; (b) Hysteresis loop of center bearing and (c) axial load variation on the center bearing

From uni-lateral tests, the normalized peak story acceleration with respect to the maximum shaking table acceleration is shown in Fig. 4. In the follows, these maximum story accelerations and displacements including those measured at the base floor will be used to correlate the experimental results with the lateral force distribution formulas given in the current design specifications such as UBC [Uniform 1997].

The lateral force distributed over the height of the structure above the isolation interface is specified by the UBC as

$$F_x = V_s \frac{w_x h_x}{\sum_{i=1}^{n} w_i h_i} \tag{1}$$

where V_s = the minimum force should be considered for the design of the superstructure above the isolation interface, which is determined from dividing the maximum base shear force transmitted by the isolation system, V_b, by a reduction factor R_I ; w_i , w_x = the weight located at story level i or x ; and h_i , h_x = the height of story level i or x above the base floor. According to the formula, two anomalies arise: (1) The formula was adopted based on an assumption that the first mode shape of an elastic multi-story fixed-base building structure can be approximately proportioned by the height of the story level above the base [Chopra 1995]. This assumption is recognized to be acceptable for most multi-story fixed-base building structures, because the design base shear force V_s is obtained by reducing the "elastic" base shear force by a factor such as R_w of UBC. However, for a base-isolated structure, the total lateral force V_s is calculated based on a reduction on the "inelastic" design base shear force V_b which is determined from an equivalent linear analysis procedure [Hwang and Chiou 1996]. The equivalent linear analysis is adopted according to the recognition that the maximum inelastic displacement response of a structure can be approximated by the maximum elastic displacement response obtained from an equivalent linear system. Therefore, the first mode shape of a base-isolated structure may not be able to be represented by the proportion of the story height as what is usually done for a fixed-base building structure; and (2) As can be seen from Eq. (1) where the index i is starting from $i = 1$, the inertia force exerting on the base floor should be excluded from the total base shear force V_b when calculating the design base shear force of the superstructure V_s. However, according to UBC, the design base shear force exerting on the superstructure is obtained by directly reducing the inelastic base shear force transmitted the isolation system V_b by an R_I factor. The inertia force on the base floor is not excluded. To illustrate these aforementioned discussions, the measured base shear force in the isolation system is substituted for V_s of Eq. (1) (i.e. R_I is set to 1) and the calculated acceleration distributions are compared with those measured from the tests in Fig. 3. From the figure, it is clear that the predicted distributions of the peak story acceleration are quite different from the measured distributions both in shape and in magnitude.

In this study, a procedure to calculate the lateral force distribution on a base-isolated building structure will be proposed in the follows. The procedure does not follow the UBC formula in which the design base shear force of the superstructure is calculated by reducing the maximum inelastic shear force of the isolation system by a

reduction factor. Instead, the lateral force distribution on the whole base-isolated structure including the base floor is calculated first based on the maximum inelastic shear force transmitted by the isolation system. Then, the lateral force exerting on the superstructure may be reduced by R_I factor if desired.

For doing so, it is intended first to ascertain whether the distribution of the maximum lateral story displacements can be used to calculate the lateral force distribution as what is usually done for an elastic fixed-base structure. The following formula is proposed to calculate the lateral force distribution and to correlate with the experimental results

$$F_x = V_b \frac{w_x \Delta_x}{\sum\limits_{i=0}^{n} w_i \Delta_i} \qquad (2)$$

where V_b = the total base shear force transmitted by the isolation system; Δ_i, Δ_x = the relative displacement of each story including the base floor to the ground. For $i=0$, w_0 = the weight of the base floor and Δ_0 = the relative lateral displacement of the isolation system to the ground which is the design displacement of the isolation system denoted as D_D in the UBC. Using Eq. (2) and the measured maximum story displacements, the lateral acceleration distribution of the test structure subjected to various ground motions can then be calculated. From Fig. 4, it is seen that the calculated maximum story accelerations compare well with the measured peak story accelerations. Therefore, it can be concluded that, even though the seismic response of a base-isolated structure is inelastic, the maximum story displacement can be used as the "mode shape" to calculate the lateral force distribution as what is usually done for an elastic fixed-base structure. One should be cautious that the weight and the lateral displacement of the base floor are involved in the above calculation using Eq. (2). However, in the practical design, these story displacements except the relative displacement (or design displacement) of the isolation system is not known prior to the calculation of the lateral force distribution. In order to facilitate the procedure for practical analysis, it is proposed that the story displacements Δ_i and Δ_x can be calculated prior to the determination of the lateral force distribution using the total base shear force V_b and a assumed lateral force distribution given by

$$f_x = V_b \frac{w_x}{\sum\limits_{i=0}^{n} w_i} \qquad (3)$$

in which f_x = the assumed lateral force distribution to calculate the lateral displacement Δ_i and Δ_x. Using Eq. (3), the story displacement can then be calculated using a simple elastic analysis. This is because the total base shear force and the maximum inelastic displacement of the isolation system predicted by Eq. (3) are exactly equal to V_b and D_D so that the stiffness of the isolation system can be represented by the effective stiffness K_{eff}. Based on Eqs. (2) and (3), the correlation between the calculated results and the experimental results is shown in Fig. 4. From this figure, it suggests that the proposed procedure be adopted for the calculation of the lateral force distribution of a base-isolated building. Once the lateral forces on the superstructure is determined,
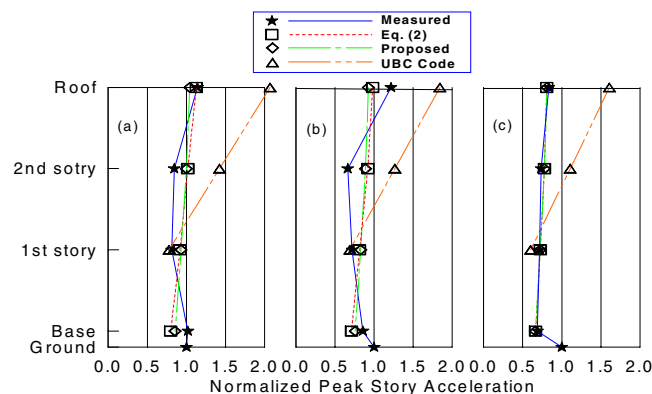
they can be reduced by R_I, if desired, to obtain the design force of the superstructure.

Figure 4: Measured and predicted normalized story acceleration (a) El Centro test; (b) Capitola test; and (c) Newhall test

3.2 Bi-lateral and Tri-Axial Tests

Among the bi-lateral and tri-axial test results, the peak story acceleration and the maximum displacement of the isolation system are of particular interest. This is because the peak story acceleration is related to the inertia force exerting on the superstructure and the maximum displacement of the isolation system is important for the design of the isolation bearings, utilities and gaps. The normalized peak story accelerations measured in the longitudinal direction reveal that the difference among the uni-lateral, bi-lateral and tri-axial test results is insignificant. This may be explained by the fact that, under bi-lateral and tri-axial excitations, the isolation bearings may yield in any lateral direction once the total shear force reaches the "yield surface" of the bearings. When the lead-rubber bearings yield, the isolation effect commences and the transmission of the ground acceleration into the superstructure is limited. Thus, the maximum longitudinal or transverse acceleration component is not necessary to be larger that of the uni-lateral tests.
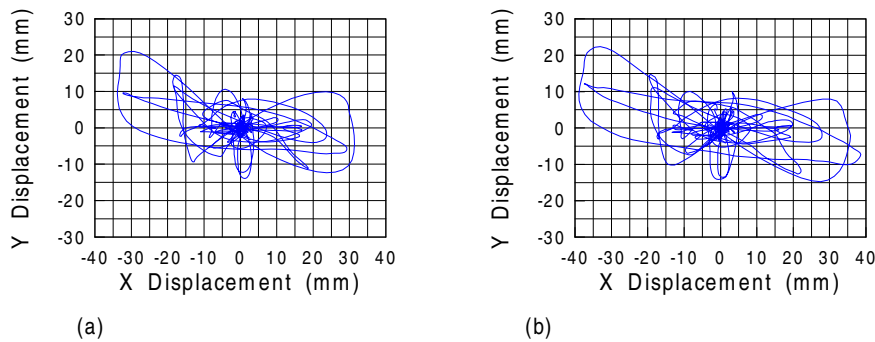
On the other hand, the maximum displacements of the isolation system determined from the uni-lateral tests, bi-lateral tests, tri-axial tests and "1.0+0.3" direction combination rule are summarized in Tables 2 and 3 in which $(U_{bx})_{max}$ = the maximum relative displacement of the isolation system measured from the uni-lateral tests in the longitudinal (X) direction; $(U_{by})_{max}$ = the maximum relative displacement of the isolation system measured from the uni-lateral tests in the transverse (Y) direction; and $(U_b)_{max}$ = the maximum relative displacement of the isolation system in any horizontal direction measured from the bi-lateral or tri-axial tests. From Table 2, it is interesting to note that the maximum displacement responses of the isolation system measured from the bi-lateral and tri-axial tests are not necessary smaller than those determined from the "1.0+0.3" direction combination rule.

Table 2: Measured maximum displacement of isolation system

Earthquake Records	Uni-Lateral		Uni-Lateral		Bi-Lateral		Tri-axial	
	$(U_{bx})_{max}$ (mm)	Occuring Time (sec)	$(U_{by})_{max}$ (mm)	Occuring Time (sec)	$(U_{bx})_{max}$ (mm)	Occuring Time (sec)	$(U_{bx})_{max}$ (mm)	Occuring Time (sec)
Capitola	30.77	5.95	19.57	5.89	38.34	5.94	42.07	5.96
Corralitos	38.74	4.96	45.88	4.96	54.28	4.66	55.81	4.68
El Centro	17.80	1.30	13.47	7.73	21.79	1.29	21.85	1.29
Kobe	29.64	5.54	24.19	5.23	33.32	5.26	33.54	5.54
Newhall	49.07	3.46	27.02	4.93	56.30	3.45	59.70	3.46
Taft	26.98	2.54	22.07	2.84	37.44	2.53	38.29	2.54

Table 3: Calculated maximum displacement of isolation system using "1.0+0.3" rule

Earthquake Records	"1.0+0.3"rule	
	$(U_{bx})_{max} + 0.3(U_{by})_{max}$ (mm)	$0.3(U_{bx})_{max} + (U_{by})_{max}$ (mm)
Capitola	36.64	28.80
Corralitos	52.50	57.50
El Centro	21.84	18.81
Kobe	36.90	33.08
Newhall	57.18	41.74
Taft	33.60	30.16

Figure 5: Displacement traces of isolation system from Capitola test (a) bi-lateral and (b) tri-axial

For example, the maximum displacements measured from the tri-axial tests of the Capitola and Taft records are about 15% larger than those obtained from the "1.0+0.3" combination rule. Therefore, the design displacement of the isolation system determined using the direction combination rule may not be conservative. In addition, it is also seen from the table that the maximum displacements of the isolation system measured from the tri-axial tests are all slightly larger than those from the bi-lateral tests. In particular, the tri-axial test with the Capitola record has generated a maximum displacement at the isolation bearings 10% larger than that of the corresponding bi-lateral test. Fig. 5 shows the comparison between the displacement traces of the isolation system measured from the bi-lateral and tri-axial tests of the Capitola record. From the comparison, the effect of vertical ground acceleration may have to be carefully considered when determining the maximum displacements of the isolation system.

4. CONCLUSIONS

Based on the three-dimensional shaking table tests of a 0.4-scale three story base-isolated steel structure, some conclusions of significance are drawn in the follows:

(1) Under a uni-lateral excitation, the effects of the axial force variation of the lead-rubber bearings have to be carefully considered for design. The axial force variation may be induced by the dead load distribution on the bearings at different locations in the building, the overturning moment of the superstructure and the excitation of the vertical ground acceleration.
(2) A method different than what have been specified in the current design practices has been proposed to calculate the lateral force distribution on the superstructure. The appropriateness of the proposed method is verified by the experiment.
(3) The results from the bi-lateral and tri-axial tests have indicated that the maximum displacement determined from the "1.0+0.3" direction combination rule may not be conservative.

ACKNOWLEDGEMENTS

REFERENCES

Al-Hussaini, T.M., Zayas, V.A. and Constantinou, M.C. (1994). "Seismic isolation of multi-story frame structures using spherical sliding isolation system." Report No. NCEER-94-0007, National Center for Earthquake Engineering Research, Buffalo, New York.

Chopra, A.K. (1995). *Dynamics of structures – theory and applications to earthquake engineering.* Prentice Hall, Englewood Cliffs, New Jersey.

Griffith, M.C., Kelly, J.M., Coveney, V.A. and Koh, C.G. (1988a). "Experimental evaluation of seismic isolation medium-rise structures subject to uplift." Report No. 88/02, Earthquake Engineering Research Center, University of California, Berkeley, California.

Hwang, J.S., Chiou, J.M. and Sheng, L.H. and Gates, J.H. (1996). "A refined model for base-isolated bridges with bi-linear hysteresis characteristics." *Earthquake Spectra*, Vol. 12, No. 2, pp. 245-274.

Hwang, J.S. and Ku. S.W. (1997). "Analytical modeling of high damping rubber bearings." *Journal of Structural Engineering, ASCE*, Vol. 123, No. 8, pp1029-1036.

Kelly, J.M. and Beucke, K.E. and Skinner, K.E. (1980). "Experimental testings of a friction damped aseismic base isolation system with fail-safe characteristics." Report No. 80/18, Earthquake Engineering Research Center, University of California, Berkeley, California.

Kelly, J.M. and Buckle, I.G. and Tsai, H.C. (1985). "Earthquake simulator testing of a base-isolated bridge deck." Report No. 85/09, Earthquake Engineering Research Center, University of California, Berkeley, California.

Guide Specifications for Seismic Isolation Design. (1999). AASHTO, Washington, D.C.

Seismic Design Specifications for Buildings (1996), Department of Interior, Taiwan.

Tyler, R.G. and Robinson, W.H. (1984). "High-strain tests on lead-rubber bearings for earthquake loading." *Bulletin of the New Zealand Society for Earthquake Engineering*, Vol. 17, No. 2, pp. 90-105.

Uniform Building Code. (1997), International Conference of Building Officials, Whittier, California.

Zayas, V.A., Low, S.S. and Mahin, S.A. (1987). "The FPS earthquake resisting system: experimental report." Report No. 87/01, Earthquake Engineering Research Center, University of California, Berkeley, California.